RSC Advances

ROYAL SOCIETY OF CHEMISTRY

www.rsc.org/advances

Journal Name

Dynamic Article Links ►

Cite this: DOI: 10.1039/c0xx00000x

www.rsc.org/xxxxxx

ARTICLE TYPE

Biocompatible graphene oxide as folate receptor-targeting drug delivery system for controlled release of anti-cancer drug

Xubo Zhao and Peng Liu*

Received (in XXX, XXX) Xth XXXXXXXXX 20XX, Accepted Xth XXXXXXXXX 20XX

DOI: 10.1039/b000000x

A novel graphene oxide (GO)-based nanocarrier has been designed for the targeting and pH-responsive controlled release of anti-cancer drug via the classic amidation of the carboxyl groups of the carboxylated graphene oxide (CG) with the amine end-groups of the functional poly(ethylene glycol) (PEG) terminated with an amino group and a folic acid group (FA-PEG-NH_2). The carboxylated graphene oxide conjugated with folate-terminated poly(ethylene glycol) (CG-PEG-FA) nanocarrier containing 44.4 wt% of the functional PEG brushes exhibit stable dispersibility in PBS media, outstanding cytocompatibility, high drug-loading capacity (for DOX of 0.3993 mg/mg) via π-π stacking interaction, perfect folate receptor-targeting and pH-activated controlled release properties, demonstrating that the nanocarrier can be a promising drug delivery system (DDS) for cancer therapy.

1. Introduction

Graphene, in which a single layer of sp^2-hybrirdized carbon atoms in a closely packed honeycomb two-dimensional (2D) crystal lattice, has attracted considerable attention due to its excellent properties and potential application since the first appearance.[1] In biomedical fields, graphene oxide (GO) and its complexes have emerged as novel substrate biomaterials, which stimulate opportunities for the development of biomedical applications including the sensing technology of DNA sequencing,[2] nanocarriers for biomedical applications,[3] and probes for cell,[4] biological imaging[5] and so on.

In recent years, enormous experiments have been done on optimizing the properties of GO to obtain new derivatives for biomedical applications.[6] Among them, grafting polymer moieties seem an efficient approach.[7] Dai et al. reported the first pioneered paper on the six-armed PEG-amine star polymer grafted GO as a novel drug nanocarrier for the water-insoluble anti-cancer drugs via hydrophobic interactions and π-π stacking interactions in 2008.[8] Meanwhile, the *in vivo* behaviors of the PEGylated GO derivatives after intravenous injection or inhalation, and uncovered the surface coating & size dependent bio-distribution and toxicology profiles were investigated. The important fundamental study has offered a deeper understanding of the *in vivo* behavior and toxicology of the functionalized graphene nanomaterials in animals, depending on their different administration routes.[9] The most intriguing property of these GO derivatives is their remarkably solubility and stability in physiological media and biocompatibility, making them promising substrate biomaterials in controlled drug delivery.

The targeting function of the drug delivery system (DDS) recently attracted considerable attention because that most of the commonly used anti-cancer drugs have serious side effects due to their unspecific actions on healthy cells.[10] By utilizing antibodies or specific ligand, the DDSs along with the therapeutic agent can selectively bind to the targeting-cells, and then be delivered to the interior of a given type of cells via the receptor mediated endocytosis.[11] Folic acid (FA), which has very high affinity for folate receptors (FRs), is one of the promising candidates for cancer-cell targeting towards several human cancer cells those over-express FRs, such as breast, ovary, lung, kidney, endometrium cancers.[12] Moreover, owing to its high stability, low cost and ability to conjugate with a large amounts of molecules, FA has received considerable attention as a targeting agent for the imaging and therapy of cancer.[13] It was also reported that the multivalent targeting effect could dramatically enhance the biological targeting ability.[14]

In the present work, the carboxylated graphene oxide conjugated with folate-terminated poly(ethylene glycol) (CG-PEG-FA) nanocarrier designed for the targeting controlled release of anti-cancer drugs by grafting the folate-terminated poly(ethylene glycol) (FA-PEG-NH_2) onto the carboxylated graphene oxide nanosheets (CG) via the classic amidation (Scheme 1). Herein, PEG brushes were introduced to the carboxylated graphene oxide nanosheets (CG), which rendered it stable under phosphate buffer saline (PBS), and folic acid (FA) moieties were attached to the CG for targeting specific cells with folate receptors. Through the transformation of the hydroxyl groups of the GO nanosheets into carboxylic acid groups, more PEG brushes as well as FA targeting moieties could be immobilized onto the functional graphene derivative. Thus, the excellent dispersibility, cytocompatibility, and targeting specificity are expected for the nanocarrier to the specific targeting controlled release of anti-cancer drugs.

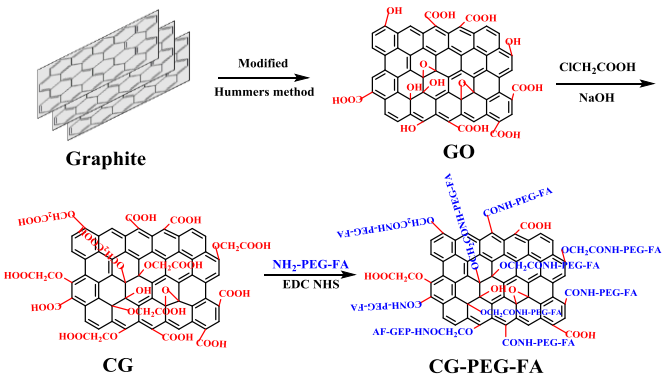

Scheme 1 Schematic illustration of the preparation of the biocompatible graphene oxide nanocarrier (CG-PEG-FA).

2. Experimental Section

2.1. Materials and reagents

Graphite powder was purchased from Huatai Chemical Reagent Co. Ltd. in Shandong, China.

Bifunctional PEG (NH_2-PEG-NH_2) and monofunctional PEG (PEG-NH_2) with DP of 2000 were provided by Beijing Kaizheng Biological Engineering Development Co., Ltd. (Beijing, China). 1-Ethyl-3-(3-dimethyl aminopropyl) carbodiimide hydrochloride (EDC·HCl) was purchased from Fluorochem. N-hydroxylsuccinimide (NHS) was purchased from Aladdin Chemistry Co. Ltd. Doxorubicin hydrochloride (DOX·HCl) was purchased from Beijing Huafeng United Technology Co. Ltd. Dimethyl sulfoxide (DMSO), folic acid (FA), potassium permanganate ($KMnO_4$), sodium nitrate ($NaNO_3$), phosphorus pentoxide (P_2O_5), potassium dichromate ($K_2Cr_2O_7$), sulfuric acid (H_2SO_4, 98%) were analytical reagent grade purchased from Tianjin Chemical Company, China. Double distilled water was used throughout.

2.2. Preparation of carboxylated graphene oxide (CG)

The graphene oxide (GO) was synthesized using a modified Hummers method from natural graphite powder.[15] Briefly, native graphite fakes (1.25 g), 1.00 g $K_2S_2O_8$, and 1.04 g P_2O_5 were added to 8.02 mL concentrated H_2SO_4 in round bottom flask, and then vigorously stirred at 82 °C for 8 h to pre-treat the graphite flakes. The product was then dried in air at ambient temperature overnight, after being washed with deionized water until neutral.

This pretreated graphite was then subjected to oxidation by the Hammers method. The pretreated graphite powder (1.01 g) was placed in two round bottom flask with $NaNO_3$ (1.00 g) and concentrated H_2SO_4 (50.1 mL) at 0 °C. $KMnO_4$ (4.01 g) was added gradually with stirring over about 1 h while keeping the temperature of the mixture around 0 °C in ice-water bath. After the mixture was stirred vigorously for 2 days at room temperature, H_2SO_4 aqueous solution (5 wt%, 100 mL) was added over about 1 h with stirring, and the temperature was kept at 98 °C. The resultant mixture was further stirred for 2 h at 98 °C. The temperature was reduced to 60 °C, subsequently, 30% H_2O_2 (3.2 mL) was added and the color of the mixture changed to bright yellow, as reported by Kovtyukhova et al[16] and the mixture was stirred for 2 h at room temperature. For purification, the mixture was centrifuged and washed with 10% HCl solution and then with deionized water to remove residual metal ions until the solution became neutral, after which individual GO nanosheets were stably dispersed in deionized water. The resulting GO nanosheets were dried at 65 °C in vacuum.

GO aqueous suspension (100 mL, 2 mg mL^{-1}) was ultrasonicated for 1 h to obtain a clear suspension. NaOH (10.00 g) and chloroacetic acid ($ClCH_2COOH$) (10.00 g) were then added to the GO suspension and ultrasonicated for another 3 h to convert the hydroxyl and epoxy groups on the GO nanosheets into the carboxyl groups. The resulting carboxylated graphene oxide (CG) suspension was neutralized, and purified by repeating the cycle of rinsing and filtration. Then, the CG suspension was dialyzed against distilled water for over 48 h to remove any ions, followed by dried at 65 °C in vacuum.[17]

2.3. Synthesis of FA-PEG-NH_2

FA (0.1301 g, 0.30 mmol), EDC (0.0606 g) and NHS (0.0338 g) were placed into a 20 mL mixture solvent of water and DMSO (1:4) in the presence of 10 mM MES. After ultrasonication, the reaction mixture was agitated 30 min to activate the carboxyl group of FA. Then, 200 μL pyridine and NH_2-PEG-NH_2 (0.6002 g, 0.30 mmol) were added into the reacting mixture and it went on to be stirred for 48 h at room temperature. After that, 4 mL deionized water was added, the insoluble substance was removed by filtration. The product was transferred to dialysis tubes (molecular weight cutoff of 1000) for about 72 h in order to removal residual folic acid, followed by lyophilization and stored at 4 °C.[18]

2.4. Conjugation of FA-PEG-NH_2 with CG

The carboxylated graphene oxide (CG) was diluted by deionized water until about 1 mg mL^{-1}. It is then ultrasonicated in 10 mg mL^{-1} FA-PEG-NH_2 for 5 min. N-(3-Dimethylaminopropyl-N'-ethylcarbodiimide hydrochloride (EDC) was then added to reach 5 mM and the solution was ultrasonicated for another 30 min, followed by adding enough EDC to reach 20 mM and stirring for 12 h. The reaction is terminated by adding mercaptoethanol. After 1 h, the final product was centrifuged and the precipitate was washed with deionized water, with several cycles of centrifugation and redispersion, to remove any excess free NH_2-PEG-FA. The obtained CG-PEG-FA was dried at 55 °C in vacuum.[18]

For comparison, the monofunctional PEG (PEG-NH_2) was also conjugated onto the CG nanosheets with the same procedure. The product (CG-PEG) was used to reveal the folate receptor-targeting function of the CG-PEG-FA nanocarrier.

2.5. DOX-loading and controlled release

The behavior of drug-loading and controlled-release performance of the CG-PEG-FA nanocarrier were assessed using a Perkin-Elmer Lambda 35 UV-vis spectrometer (Perkin-Elmer Instruments, USA) at room temperature. Standard curves for doxorubicin was prepared by measuring the UV absorbance of a series of doxorubicin solutions with known concentration in PBS. The cumulative release (%) of drug at a particular time (*t*) can be calculated according to:

Cumulative release (%) = cumulative amount released/ total mass loaded × 100%

For the drug-loading, the solutions of doxorubicin (DOX) (1.0 mg mL^{-1}) were prepared in deionized water. The CG-PEG-FA nanocarrier (~10.0 mg) was added into 5.0 mL doxorubicin solution (pH 5.0, 6.5, 7.4 or 8.5, respectively) for drug loading. After being swung by table concentrator for 24 h, the different doxorubicin-loaded CG-PEG-FA nanocarriers (CG-PEG-FA/DOX) were centrifuged to remove the excess DOX. Compared with the CG-PEG-FA nanocarrier, doxorubicin (DOX) loaded CG nanocarrier was researched at pH 7.4 of the DOX solution. The drug concentration in the supernatant solution was monitored using an ultraviolet (UV) spectrophotometer at 233 nm to assess the drug-loaded capacities. The drug-loading capacities of the GO and the CG-PEG-FA nanocarriers were calculated from the drug concentrations before and after loading.

As for their controlled release, the dispersion of the CG-PEG-FA/DOX (10 mL) in phosphate-buffered saline (PBS at pH 7.4, 6.5 or 5.0) was transferred to dialysis tubes (molecular weight cutoff of 10 000), and immersed into 120 mL PBS at 37 °C at pH 7.4, 6.5 or 5.0, respectively. Aliquots (5.0 mL) of solution were removed at certain intervals, and the drug concentrations in the dialysates were analyzed using a UV spectrophotometer to assess the cumulative release of the drug-loaded CG-PEG-FA nanocarrier. 5.0 mL fresh PBS was added after each sampling to keep the total volume of the solution constant. The cumulative release was expressed as the total percentage of drug released from the drug-loaded CG-PEG-FA nanocarrier and was transported through the dialysis membrane over time.

The drug release data obtained from the in vitro release study was analyzed for the rate of release, using the Higuchi drug release equation given below:

$$M_t = k \cdot t^{1/2}$$

where M_t is the amount of drug release at time t, and k is the rate constant.

When a plot of cumulative drug release of $t^{1/2}$ yields a straight line with a slope which possesses a value ≥1, the particular system is considered to follow Higuchi kinetics of drug release.[19]

$$M_t/M_\infty = k \cdot t^n$$

where M_t/M_∞ is the fraction of drug release at time t; k is a constant comprising the structural and geometric characteristics of the controlled release system; and n, the release exponent, is a important parameter that depends on the release mechanism and is thus used to characterize it.[20] Thus, the Korsmeyer-Peppas equation has two distinct physical realistic meanings in the two special cases of n = 0.5 (indicating diffusion-controlled drug release) and n = 1.0 (indicating swelling-controlled drug release). The n values between 0.5 and 1.0 can be regarded as an indicator for the superposition of both phenomena (anomalous transport). For the determination of the exponent n, the portion of the release curve where $M_t/M_\infty < 0.6$ should be used. The n value could be obtained from the slope of a plot of log M_t/M_∞ *versus* log t.[21] Therefore in conjunction with the Higuchi model, the Korsmeyer-Peppas relation was also utilized to establish a drug release mechanism for the drug-loaded CG-PEG-FA nanocarrier in the present work.

2.6. Cell toxicity assays

MTT (3-(4, 5-dimethylthiazol-2-yl)-2, 5-diphenyltetrazolium bromide) assay was performed to evaluate the cytocompatibility and targeting-specificity of the CG-PEG-FA nanocarrier with HepG2 cells (well-known model of parenchymal cells in liver with over-expressing FA receptors (folate receptor-positive cells)) and the liver sinusoidal endothelial cells (LSEC) with DOX as the model drug, respectively.

For the MTT assay, the cells were seeded into 96-well plates at densities of 1×10^5 cells per well for 24 h. Then, the CG-PEG-FA nanocarrier with different concentrations, drug-loaded CG-PEG-FA and CG-PEG nanocarriers, and DOX were added to the cells and incubated for 48 h. Thereafter, the cells were washed three times with phosphate buffered saline (PBS) and processed for the MTT assay to determine the cell viability. 100 uL pH 7.4 PBS solution containing 20 uL 5 mg mL^{-1} MTT was added to each well, and incubated for an additional 4 h, following drew the medium. Cell bound dye was dissolved with 100 uL DMSO in each well cell culture plate and swung by table concentrator for 20 min, The absorbance of each well was read on a microplate reader using a test wavelength of 490 nm.

2.7. Characterization

The biocompatible CG-PEG-FA nanocarrier was characterized with a Bruker IFS 66 v/s infrared spectrometer (Bruker, Karlsruhe, Germany) was used for the Fourier transform infrared (FT-IR) spectroscopy analysis in the range of 400−4000 cm^{-1} with a resolution of 4 cm^{-1}. The KBr pellet technique was adopted to prepare the sample for recording the IR spectra.

Raman spectra were carried out with a Horiba Jobin-Yvon LabRAM HR 800 UV apparatus using an excitation laser with a wavelength of 532 nm.

Thermogravimetric analysis (TGA) results were obtained with a TA Instrument 2050 thermogravimetric analyzer at a heating rate of 10 °C min^{-1} from 25 to 800 °C at nitrogen atmosphere.

The morphologies of the biocompatible CG-PEG-FA nanocarrier were characterized with a JEM-1200 EX/S transmission electron microscope and SPA-300HV atomic force microscope. The samples were dispersed in water and then deposited on a copper grid covered with a perforated carbon film and deposited silicon wafer, followed by dried at 45 °C in vacuum, respectively.

3. Results and Discussion

The synthetic route for the preparation of the CG-PEG-FA nanocarrier was shown schematically in Scheme 1, containing the three steps: preparation of the GO nanosheets, carboxylating the GO into CG nanosheets, and conjugating FA-PEG-NH_2 to the CG nanosheets via the classic amidation between the -NH_2 groups of FA-PEG-NH_2 and the -COOH groups of the CG. It is well known that the GO contains sp^2 hybridized carbons on the aromatic network. The large π conjugated structure of the designed biocompatible and targeting-specific CG-PEG-FA nanocarrier can form π-π stacking interaction and hydrophobic interaction with the aromatic drugs such as doxorubicin (DOX). So the designed CG-PEG-FA nanocarrier is expected to be potential specific targeting controlled release of anti-cancer drugs.

3.1. Preparation of CG-PEG-FA

FA-PEG-NH_2 was synthesized via the amidation of the NH_2-PEG-NH_2 with FA, revealed by the appearance of the absorbance at 1645 cm^{-1} in the FT-IR spectra (Fig. S1, ESI †).

The GO was synthesized using a modified Hummers method from natural graphite powder[15] and could be proved by the appearance of the absorbance peak at 1706 cm^{-1} of the C=O stretch band of the carboxyl groups (Fig. 1). The absorbance peaks at 1041, 1391, 1623 and 1706 can be attributed to C–O stretching (epoxy or alkoxy), O–H stretching (carboxyl), C=C skeletal vibrations of unoxidized graphite domains, C=O in carboxylic acid and carbonyl moieties, respectively.

There are plentiful hydroxyl and epoxy groups in the GO nanosheets. It is necessary to convert these groups into COOH groups to improve the aqueous solubility and reaction sites of the graphene derivatives and to facilitate chemical binding of the functional PEG to the CG via EDC chemistry. In present study, the hydroxyl and epoxy group of the GO were converted into COOH groups by mixing the GO with $ClCH_2COOH$ under strong alkaline conditions according to the literature.[17] It is interestingly that the color of the GO suspension changed from dark-brown to black during the conversion process, it may be due to partial reduction of the GO under strong alkaline conditions.[22] The presence of -CH_2COOH groups in the carboxylated grapheme oxide (CG) was confirmed by FT-IR spectra (Fig. 1). A new peak is found in the IR spectrum of the CG at 1088 cm^{-1} of the stretching vibration of the C−O−C groups, compared with the grapheme oxide (GO). It indicated that the hydroxyl and epoxy groups of the GO were successfully converted into the -COOH groups. And the peak at 1706 cm^{-1} corresponding to C=O of –COOH on the GO shifted to 1700 cm^{-1} of the CG due to –CH_2COOH portion grew in quantity in the CG.

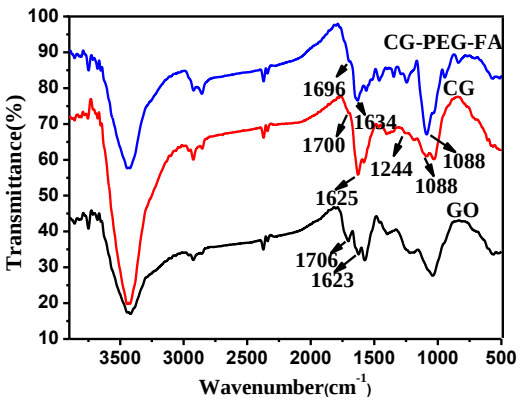

Fig. 1. FT-IR spectra of the GO, CG and CG-PEG-FA nanosheets measured in KBr pellets.

Then a hydrophilic biocompatible polymer, PEG conjugated with targeting ligand (folic acid (FA)) was synthesized for the surface modification of the CG nanosheets to improve their cytocompatibility and targeting specificity. The presence of FA moieties in the FA-PEG-NH_2 was confirmed by FT-IR measurements. The characteristic peak of FA at 1585 cm^{-1} could be clearly observed in Fig. S1, ESI †, which is slightly shifted in the FT-IR spectrum of FA-PEG-NH_2. Also, the clear peak at 1645 cm^{-1} corresponding to the characteristic peak of N–O in the FT-IR spectrum of the folic acid active ester was observed.[23] This finding suggested that FA was successfully conjugated with the NH_2-PEG-NH_2.

After the CG was conjugated with FA-PEG-NH_2, the peak at 1700 cm^{-1} shifted to 1696 cm^{-1} in the CG-PEG-FA spectrum due to the hydrogen bond was formed between carboxyl group of folic acid moieties and carboxyl group on the GC. At the same time, the peak at 1088 cm^{-1} corresponding to the C–O–C characteristic absorbance might emerge in the FT-IR spectra of the biocompatible and specific targeting CG-PEG-FA nanocarriers. Meanwhile, the conjugation of FA-PEG-NH_2 onto the CG through the formation of an amide bond was confirmed by the strong NH-CO stretching vibration (1634 cm^{-1}). These results suggested that the biocompatible and specific targeting CG-PEG-FA nanocarrier was successful designed via covalent attachment of the functional polymer brushes.

Two new absorbance bands at 283 and 380 nm, which can't be seen in the UV-vis absorption spectrum of the CO nanosheets, appeared in that of the CG-PEG-FA (Fig. 2), attributing to the characteristic absorbance of the pterin ring in FA.[24] However, the GO only displayed a small absorbance peak at about 233 nm due to the π - π^* of C=C.[25] It also verified the successful grafting of the folate-terminated poly(ethylene glycol) (FA-PEG-NH_2) onto the CG nanosheets via the facile amidation (Scheme 1).

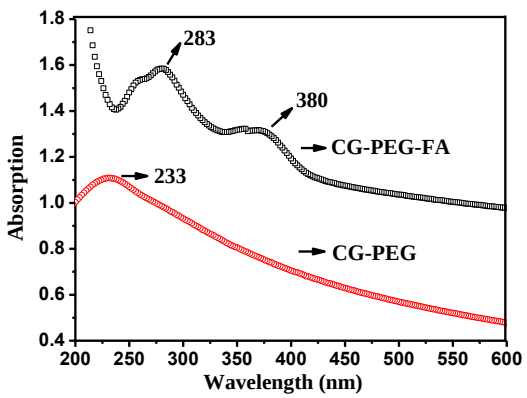

Fig. 2. UV/Vis spectra of the GO and CG-PEG-FA nanosheets in their aqueous dispersions.

The TGA curves of the functional graphene nanosheets are shown in Fig. 3. The GO showed a large weight loss (more than 30%) at the temperature lower than 200°C, attributed to the removal of the water that is held in the material, and the functional groups (–OH and –COOH), from the GO.[26] As for the CG nanosheets, the weight loss in the temperature range decreased to about 15%, and a sharp weight loss near 20% occurred around 200 °C, resulted from the decomposition of the organic groups (hydroxyl, epoxy and carboxyl groups) of the CG nanosheets. [27]

There was a 60 wt% weight loss at 450 °C for the CG-PEG-FA, whereas the GO and CG nanosheets exhibited weight losses of 37 wt% and 46 wt%, respectively. Moreover, the weight loss about 40 wt% occurred in 220-450 °C in the curve of the CG-PEG-FA, it may be due to the decomposition of the FA-PEG-NH_2 polymer brushes on the CG-PEG-FA nanocarrier. So it also can calculate that the CG-PEG-FA nanocarrier contained about 44.4 wt% FA-PEG-NH_2 polymer moieties from the TGA results (Fig. 2). The

value is twice as the the result by grafting PEG_{400} onto the GO directly,[28] although PEG_{2000} was used in the present work, for which the bigger steric hindrance resulted from the higher molecular weight hinder the grafting. It revealed that the carboxylation of the GO is an efficient method to increase the functionalization degree of the GO nanosheets.

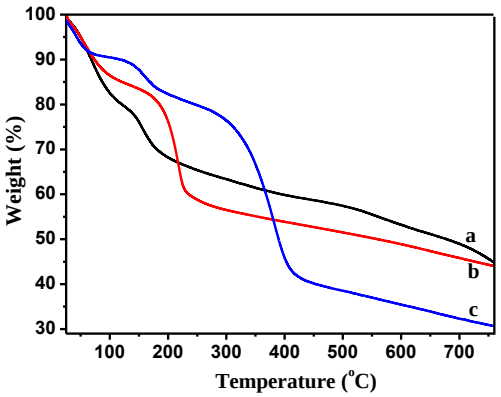

Fig. 3. TGA curves of the GO (a), CG (b) and CG-PEG-FA (c) nanosheets in N_2 atmosphere.

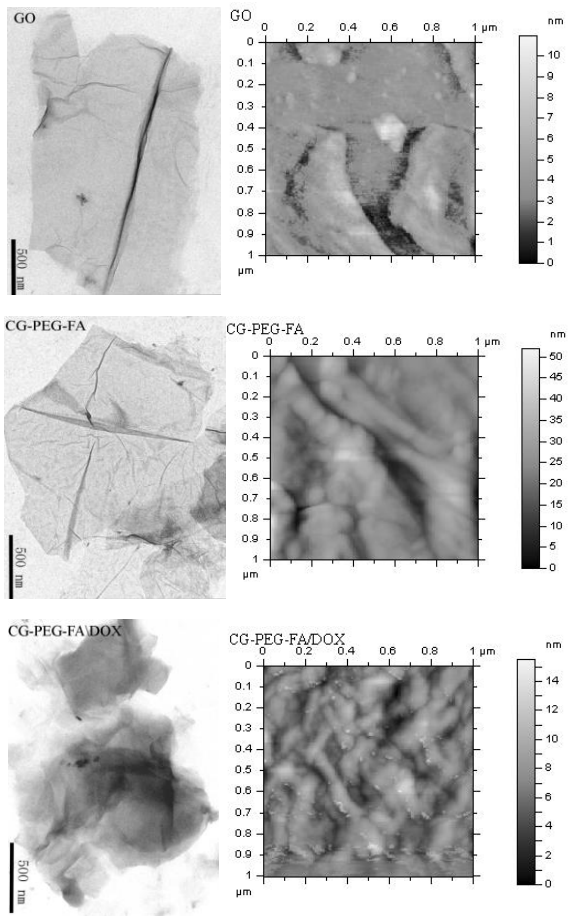

Fig. 4. TEM and AFM images of the GO, CG-PEG-FA, CG-PEG-FA/DOX.

Transmission electron microscopy (TEM) and atomic force microscopy (AFM) images (Fig. 4) provide the morphological information on the GO and the CG-PEG-FA nanocarrier. A typical TEM image of the GO showed the see-through flaky material with the size less than 2 μm in lateral width. It is the characteristic of the GO as a single or two layered sheets.[29]

A large number of new groove-like and ridge-like morphologies were found in the AFM image of the CG-PEG-FA compared with the GO. Graphene oxide (GO) sheets existed with very sharp edges and flat surface. In contrast, the edges of the CG-PEG-FA nanocarrier appeared relatively groove-like and some ridge-like structures were observed on the surfaces, which were formed by the polymer wrapping and folding on the surfaces.[6] It also revealed that the functional PEG brushes had been successfully grafted onto the surface of the GO nanosheets.

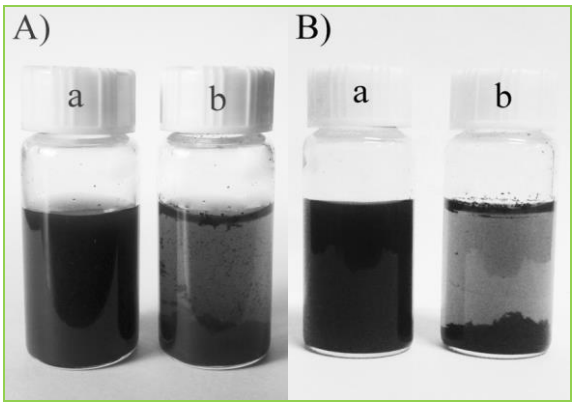

Fig. 5. Digital photos of the pH 7.4 PBS dispersions of the CG-PEG-FA (a) and the CG (b) nanosheets after stopping ultrasonication for A) 0.5 h, and B) 48 h. The concentration of all samples was around 0.4 mg mL^{-1}.

Owing to the incorporation of FA-PEG-NH_2 polymer brushes, the CG-PEG-FA can be readily dissolved in phosphate buffer saline (PBS, pH=7.4) with the aid of ultrasonication. Fig. 5A and B showed the dispersion state of the GO and the CG-PEG-FA in phosphate buffer saline (PBS) at the same concentration (0.4 mg mL^{-1}) after 0.5 and 48 h at 37 °C, respectively. It was found that GO could not be well dispersed in PBS (pH 7.4) and precipitated after stopping ultrasonication for 0.5 h. Interestingly, the solubility of the CG-PEG-FA nanocarrier in PBS (pH 7.4) was good due to the benign solubility of the –PEG-FA polymer brushes. The excellent stability of dispersion in PBS (pH 7.4) at 37 °C encouraged us to explore the applications of CG-PEG-FA nanocarriers in controlled loading and drug delivery.

3.2. DOX-loading

The drug-loading property of the biocompatible and specific targeting CG-PEG-FA nanocarrier was investigated at different pH value (5.0, 6.5, 7.4 or 8.5) at 37 °C with model hydrophobic anti-cancer drug (doxorubicin (DOX)), determined by UV-vis spectroscopy at 233 nm. The DOX-loading capacity was found to be 0.2977±0.0120, 0.3483±0.0088, 0.3993±0.0153, and 0.3672±0.0055 mg/mg from the different pH values of 5.0, 6.5, 7.4 or 8.5 at 37 °C, respectively. Thus it can be seen that the highest loading capacity is observed at the neutral condition, rather than acidic or basic conditions. The pH-dependent loading may be due to

the different the solubility of DOX under different pH conditions.[30] Its high DOX-loading capacity also could be seen in the AFM image of the DOX loaded CG-PEG-FA nanocarrier (CG-PEG-FA/DOX), in which there are many surface protuberances on the groove-like and ridge-like nanosheets (Fig. 4).

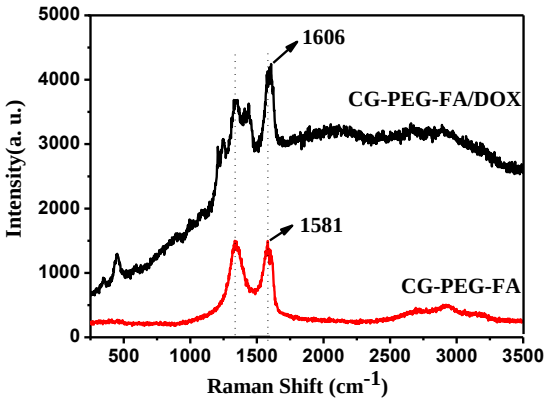

Fig. 6. Raman spectra of the CG-PEG-FA/DOX and CG-PEG-FA at a laser excitation wavelength of 532 nm.

The highest loading capacity of the CG-PEG-FA was lower than that of the GO of 0.4546±0.0287 mg/mg under the same condition (Fig. S2B, ESI †). It may be due to that the lager functional PEG brushes on the CG reduced the interaction between the drug molecules and the nanocarrier. In the Raman analyses (Fig. S6), the G band (1581 cm^{-1}) corresponding to the sp^2 hybridized carbon shifted to 1606 cm^{-1} after the drug-loading, indicated that the drug-loading might be conducted via the π-π stacking interaction between DOX and the aromatic structure on the CG-PEG-FA.[31] It also could explain the drug-loading difference between the GO and the CG-PEG-FA.

3.3. Controlled release

Then the drug release behaviors of the CG-PEG-FA/DOX were investigated in PBS solutions with different pH values at 37 °C. The cumulative release at pH 7.4, 6.5 and 5.0 were calculated to be about 12.86%, 16.52%, and 41.42%, respectively (Fig. 7). The cumulative release rate at pH 7.4 and 6.5 reached 6.43% and 8.01% within 5.5 h, respectively, while that at pH 5.0 reached 15.74%. That is to say, the CG-PEG-FA/DOX nanocarrier has favorable release rate in acidic phosphate buffer solutions, due to the higher solubility of DOX in acidic media. So it could be concluded that the drug release should be governed simultaneously by the saturated solubility of DOX,[32] and the designed CG-PEG-FA possesses the pH-activated controlled release characteristics.

The DOX release data was analyzed using the Higuchi and Korsmeyer-Peppas equations. The release rates *k* and *n* of each model were calculated by linear regression analysis. Coefficients of correlation (R^2) were used to evaluate the accuracy of the fitting. The plots for the Higuchi equation of the CG-PEG-FA/DOX nanocarrier (pH 7.4, 6.5 or 5.0. at 37°C) resulted in linearity with an R^2 value of 0.9421, 0.9762 and 0.9524, and a *k* value of 0.1542, 0.2004 and 0.5592 (Fig. S3 ESI †), respectively. However, the *k* values of the Higuchi equation were inferior to 1, so the Fickian diffusion could not be used to describe the drug release of the CG-PEG-FA/DOX nanocarrier at pH 7.4. But even more crucial, the plot of the Korsmeyer-Peppas equation were used to described DOX release mechanism of the CG-PEG-FA/DOX nanocarrier in PBS (pH 7.4, 6.5, 5.0. at 37°C) (Fig. S3 ESI †). The plots for the Korsmeyer-Peppas equation of the CG-PEG-FA/DOX resulted in linearity with an R^2 value of 0.9705, 0.9828 and 0.9840, and an *n* value of 0.2644, 0.1605 and 0.1674, respectively. The Korsmeyer-Peppas equation yielded comparatively good linearity (R^2 = 0.9705, 0.9828 and 0.9840) and perfect release exponent (*n* = 0.2644, 0.1605 and 0.1674). The results revealed its release mechanism was diffusion-controlled drug release.[33]

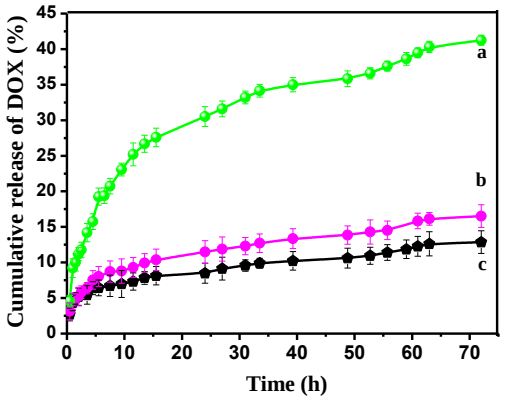

Fig. 7. Cumulative release of DOX from the DOX-loaded CG-PEG-FA at phosphate buffer (pH 5.0) (a), (pH 6.5) (b) and (pH 7.4) (c) at 37°C.

3.4. Cytotoxicity and targeting specificity

The cytocompatibility of the CG and the CG-PEG-FA was evaluated in HepG2 cells using MTT assays. Dose-response study was also performed by exposing HepG2 cells to various concentrations of the two nanosheets. As shown in Fig. 8(A), excellent cyto-compatibility was showed by increasing the concentration of the CG-PEG-FA with cell viability of 98.8-104.7% from 0 to 50 ug/mL after 48 h while the viability decreased from 102.7% to 86.9% with the tested concentration of the CG nanosheets after 48 h of incubation. It indicated that the CG-PEG-FA has low cytotoxicity on HepG2 cells in these concentrations, due to the functional PEG brushes.[8,34]

To evaluate the folic acid (FA) group-mediated targeting function of the CG-PEG-FA, the CG-PEG-FA/DOX and the CG-PEG/DOX (with the DOX-loading capacity of 0.4015±0.0114 mg/mg at pH 7.4) were used for the *in vitro* study with HepG2 cells and LSEC. The two graphene-based nanocarriers had the similar structure except that the PEG brushes on the CG-PEG-FA were terminated with the FA moieties. The DOX-loading capacity of the CG-PEG-FA was 99.5% of the CG-PEG under the same drug-loading condition, and the marginal difference between the two nanocarriers was caused by the FA moieties in the CG-PEG-FA. So it could be concluded that the two nanocarriers must have the same drug-loading mechanism, as well as the releasing mechanism.

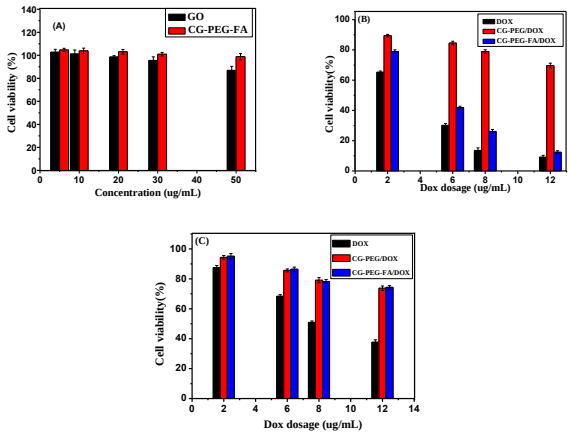

Fig. 8. Cell viability assay in HepG2 cells of the GO and CG-PEG-FA (A) and cell viability assay of the CG-PEG/DOX, the CG-PEG-FA/DOX and the free DOX with various concentrations (2, 6, 8 and 12 μg/mL) to HepG2 cells (B) and LSEC (C) at 37 °C for 48 h, respectively. Cell viability (%) was determined by the MTT assay.

As shown in Fig. 8 (B), the anticancer activity tests showed that the free DOX and the CG-PEG-FA/DOX displayed similar anticancer activity toward HepG2 cell lines. In the absence of folic acid, the anticancer activity of the CG-PEG/DOX was dramatically decreased. The order of efficacy as a killing agent is the free DOX, then the targeting-specific CG-PEG-FA/DOX, and finally the nontargeting-specific CG-PEG/DOX. It revealed that the targeting-specific CG-PEG-FA/DOX showed obvious cell inhibition than the nontargeting-specific CG-PEG/DOX, mainly attributed to the plentiful FA receptors (FRs) on the surface of the tumor cells. Therefore, we can deduce that the DOX-loaded CG-PEG-FA biocompatible and targeting-specific nanocarriers shows no obvious difference in therapeutic effects against cancer cells as compared with the free DOX, but shows much lower cyto-toxicity.

As for the LSEC lines, a type of human liver sinusoidal endothelial cells, the targeting-specific CG-PEG-FA/DOX and the nontargeting-specific CG-PEG/DOX displayed similar anticancer activity, much lower than that of the free DOX with increasing the DOX dosage (Fig. 8(C)). With the same DOX dosage of 12 μg/mL, the relative cellular viability of the CG-PEG-FA/DOX and the CG-PEG/DOX reached about 74% within 48 h, which was much higher than that of the free DOX (37.65%). It meant that the cell toxicity of DOX had been decreased significantly by the two drug carriers. Furthermore, the similar anti-tumor efficacy of the two nanocarriers indicated that the folic acid groups had no targeting-specificity to the normal cells. These results demonstrated that folic acid segments played an important role of receptor-mediated specificity for selective killing of cancer cells.[35]

Conclusions

In summary, an efficient approach was developed to decorate the carboxylated graphene oxide (CG) nanosheets with functional poly(ethylene glycol) (PEG) terminated with an amino group and a folic acid group (FA-PEG-NH_2) via the classic amidation to synthesize a novel nanocarrier (CG-PEG-FA) as biocompatible, targeting and controlled DDS. The CG-PEG-FA contained about 44.4 wt% of the functional PEG brushes, which rendered it stable dispersibility in PBS media, and the attached FA moieties made it target specifically cells with folate receptors (FRs). Particularly, the CG-PEG-FA possessed a superior binding capability for DOX of 0.3993 mg/mg at pH value 7.4, via π-π stacking interaction revealed by Raman. Moreover, the DOX-loaded CG-PEG-FA nanocarrier (CG-PEG-FA/DOX) exhibited pH-activated controlled release. Versatility Higuchi and simplicity Korsmeyer-Peppas equations demonstrated that diffusion was the primary governing force for the drug release from the CG-PEG-FA/DOX in SBF. At last, the MTT assay indicated the CG-PEG-FA has outstanding cytocompatibility and targeting-specificity of cancer cells via over-expressing FRs. This work demonstrated the viability of utilizing functionalized GO with good solubility and stability, biocompatibility and targeting specificity as the drug nanocarrier for controlled loading and folate receptor-targeting drug delivery of the anti-cancer drugs, which may have potential clinical advantages pertaining to increase therapeutic efficacy.

Acknowledgments

This project was granted financial support from the National Nature Science Foundation of China (Grant No. 20904017) and the Program for New Century Excellent Talents in University (Grant No. NCET-09-0441).

Notes and references

State Key Laboratory of Applied Organic Chemistry and Key Laboratory of Nonferrous Metal Chemistry and Resources Utilization of Gansu Province, College of Chemistry and Chemical Engineering, Lanzhou University, Lanzhou 730000, China. Fax./Tel: 86 0931 8912582; E-mail: pliu@lzu.edu.cn.

† Electronic Supplementary Information (ESI) available: The FTIR spectra of the NH_2-PEG-NH_2 and NH_2-PEG-FA, the DOX-loading capacity of the CG-PEG-FA nanocarrier at different pH values, and the kinetics models of the drug release performance. See DOI: 10.1039/b000000x/

1 A. K. Geim and K. S. Novoselov. *Nature Mater*., 2007, **6**, 183.
2 F. Haque, J.H. Li, H.-C. Wu, X.-J. Liang and P.X. Guo. *Nano Today*, 2013, **8**, 56.
3 K. Yang, J.M. Wan, S. Zhang, Y.J. Zhang, S.-T. Lee and Z. Liu. *ACS Nano*, 2011, **5**, 516.
4 Y. Wang, Z.H. Li, D.H. Hu, C.T. Lin, J.H. Li and Y.H. Lin. *J. Am. Chem. Soc.*, 2010, **132**, 9274.
5 K. Yang, L.Z. Feng, X.Z. Shi and Z. Liu. *Chem. Soc. Rev.*, 2013, **42**, 530.
6 Y. Wang, Z.H. Li, J. Wang, J.H. Li and Y.H. Lin. *Trend Biotechnol.*, 2011, **29**, 205; Y.Z. Pan, H.Q. Bao, N.G. Sahoo, T.F. Wu and L. Li. *Adv. Funct. Mater.*, 2011, **21**, 2754.
7 H. Zhang, G. Gruner and Y. Zhao. *J. Mater. Chem. B*, 2013, **1**, 2542.
8 Z. Liu, J.T. Robinson, X.M. Sun and H.J. Dai. *J. Am. Chem. Soc.*, 2008, **130**, 10876.
9 K. Yang, H. Gong, X.Z. Shi, J.M. Wan, Y.J. Zhang and Z. Liu. *Biomaterials*, 2013, **34**, 2787.
10 S.S. Dharap, Y. Wang, P. Chandna, J.J. Khandare, B. Qiu, S. unaseelan, P.J. Sinko, S. Stein, A. Farmanfarmaian and T. Minko. *Proc. Natl. Acad. Sci. USA*, 2005, **102**, 12962.
11 J.M. Rosenholm, A. Meinander, E. Peuhu, R. Niemi, J.E. Eriksson, C. Sahlgren and M. Linde. *ACS Nano*, 2009, **3**, 197.
12 P.S. Low, W.A. Henne and D.D. Doorneweerd. *Acc. Chem. Res.*, 2008, **41**, 120; J.F. Ross, P.K. Chaudhuri and M. Ratnam. *Cancer*, 1994, **73**, 2432.

13 J. Sudimack and R.J. Lee. *Adv. Drug Deliv. Rev.*, 2000, **41**, 147; P.S. Low, W.A. Henne and D.D. Doorneweerd. *Acc. Chem. Res.*, 2008, **41**, 120; L. Zhang, J. Xia, Q. Zhao, L. Liu and Z. Zhang. *Small*, 2010, **6**, 537.
14 S. Hong, P.R. Leroueil, I.J. Majoros, B.G. Orr, J.R. Baker Jr. and M.M.B. Holl. *Chem. Biol.*, 2007, **14**, 107.
15 W.S. Hummers and R.E. Offeman, *J. Am. Chem. Soc.*, 1958, **80**, 1339.
16 N.I. Kovtyukhova, P.J. Ollivier, B.R. Martin, T.E. Mallouk, S.A. Chizhik, E.V. Buzaneva and A.D. Gorchinskiy. *Chem. Mater.*, 1999, **11**, 771.
17 Z. Hu, J. Li, S.J. Zhao, N. Li, Y.F. Wang, F. Wei, L. Chen and Y.D. Huang. *J. Mater. Chem. B*, 2013, **1**, 5003.
18 X.Y. Yang, G.L. Niu, X.F. Cao, Y.K. Wen, R. Xiang, H.Q. Duan, Y.S. Chen. *J. Mater. Chem.*, 2012, **22**, 6649.
19 T. Higuich. *J. Pharm. Sci*., 1961, **50**, 874.
20 R.W. Korsmeyer, R. Gurny, E.M. Doelker, P. Buri and N.A. Peppas. *Int. J. Pharm.*, 1983, **15**, 25.
21 J. Siepmann and N.A. Peppas. *Adv. Drug Deliv. Rev.*, 2001, **48**, 139.
22 X. Fan, W. Peng, Y. Li, X. Li, S. Wang, G. Zhang and F. Zhang. *Adv. Mater*., 2008, **20**, 4490.
23 X.Y. Yang, Y.S. Wang, X. Huang, Y.F. Ma, Y. Huang, R.C. Yang, H.Q. Duan and Y.S. Chen. *J. Mater. Chem.*, 2011, **21**, 3448.
24 T. Kato, T. Matsuoka, M. Nishii, Y. Kamikawa, K. Kanie, T. Nishimura, E. Yashima and S. Ujiie. *Angew. Chem. Int. Ed.*, 2004, **43**, 1969.
25 Z.T. Luo, Y. Lu, L.A. Somers and A.T.C. Johnson. *J. Am. Chem. Soc.*, 2009, **131**, 898.
26 D. Dikin, S. Park, W. Cai, S.L. Mielke and R.S. Ruoff. *J. Phys. Chem. C.*, 2008, **112**, 20264.
27 J. Shen, Y. Hu, C. Li, C. Qin and M. Ye. *Small*, 2009, **5**, 82.
28 S.P. Zhang, P. Xiong, X.J. Yang and X. Wang. *Nanoscale*, 2011, **3**, 2169.
29 N. Pan, D.B. Guan, Y.T. Yang, Z.L. Huang, R.B. Wang, Y.D. Jin and C.Q. Xia. *Chem. Eng. J.*, 2014, **236**, 471.
30 X.Y. Yang, X.Y. Zhang, Z.F. Liu, Y.F. Ma, Y. Huang and Y.S Chen. *J. Phys. Chem. C*, 2008, **112**, 17554.
31 Q.Yao, L.D. Chen, W.Q. Zhang, S.C. Liufu and X.H. Chen. *ACS Nano*, 2010, **4**, 2445; C. Yang, P. Liu, P.C. Du and X. Wang. *Electrochim. Acta*, 2013, **105**, 53.
32 X.B. Zhao, P.C. Du and P. Liu. *Mol. Pharmaceutics*, 2012, **9**, 3330.
33 J. Siepmann and N.A. Peppas. *Adv. Drug Deliv. Rev.*, 2001, **48**, 139.
34 F.F. Cheng, W. Chen, L.H. Hu, G. Chen, H.T. Miao, C.Z. Li and J.J. Zhu. *J. Mater. Chem, B*, 2013, **1**, 4956; J.T. Robinson, S.M. Tabakman, Y.Y. Liang, H.L. Wang, H.S. Casalongue, D. Vinh and H.J. Dai. *J. Am. Chem. Soc.*, 2011, **133**, 6825.
35 H.X. Wu, G. Liu, S.J. Zhang, J.L. Shi, L.X. Zhang, Y. Chen, F. Chen and H.R. Chen. *J. Mater. Chem.*, 2011, **21**, 3037; P.C. Du, J. Zeng, B. Mu and P. Liu. *Mol. Pharmaceutics*, 2013, **10**, 1705; P.C. Du, H.Y. Yang, J. Zeng and P. Liu. *J. Mater. Chem. B*, 2013, **1**, 5298; X.M. Sun, Z. Liu, K. Welsher, J.T. Robinson, A. Goodwin, S. Zaric and H.J. Dai. *Nano Res.*, 2008, **1**, 203; L.M. Zhang, J.G. Xia, Q.H. Zhao, L.W. Liu and Z.J. Zhang. *Small*, 2010, *6*, 53; Y. Yang, Y.M. Zhang, Y. Chen, D. Zhao, J.T. Chen and Y. Liu. *Chem. Eur. J.*, 2012, *18*, 4208.